Available online at www.sciencedirect.com
ScienceDirect
Journal of Computational Physics 227 (2007) 1523–1543
JOURNAL OF COMPUTATIONAL PHYSICS
www.elsevier.com/locate/jcp

Poloidal–toroidal decomposition in a finite cylinder. I: Influence matrices for the magnetohydrodynamic equations

Piotr Boronski *, Laurette S. Tuckerman

LIMSI-CNRS, BP 133, 91403 Orsay, France

Received 7 May 2007; received in revised form 25 August 2007; accepted 28 August 2007
Available online 6 September 2007

Abstract

The Navier–Stokes equations and magnetohydrodynamics equations are written in terms of poloidal and toroidal potentials in a finite cylinder. This formulation insures that the velocity and magnetic fields are divergence-free by construction, but leads to systems of partial differential equations of higher order, whose boundary conditions are coupled. The influence matrix technique is used to transform these systems into decoupled parabolic and elliptic problems. The magnetic field in the induction equation is matched to that in an exterior vacuum by means of the Dirichlet-to-Neumann mapping, thus eliminating the need to discretize the exterior. The influence matrix is scaled in order to attain an acceptable condition number.

Keywords: Poloidal–toroidal; Influence matrix; Magnetohydrodynamics; Divergence-free; Finite cylinder; Dirichlet-to-Neumann mapping; Compatibility conditions; Matrix conditioning

1. Motivation and governing equations

The requirement that velocity and magnetic fields be solenoidal, i.e. divergence-free, represents one of the most challenging difficulties in hydrodynamics and in magnetohydrodynamics [1–10]. For the velocity field, this condition is the fundamental approximation used in incompressible fluid dynamics. For the magnetic field, this condition is the statement of the non-existence of magnetic monopoles.

Two main approaches exist for imposing this requirement. The first is to use three field components and to project three-dimensional fields onto a divergence-free field. In an incompressible fluid, the pressure serves to counterbalance the nonlinear term which is the source of the divergence in the Navier–Stokes equations; the pressure also plays this role numerically. The divergence of the Navier–Stokes equations is taken, leading to a Poisson problem for the pressure. However, the boundary conditions on the equations for $(\mathbf{u}, p)$ involve only the velocity, leading to coupling between the equations to be solved for $\mathbf{u}$ and p [3,4]. The coupled equations can be solved in several stages by a Green's function or influence matrix method [3,5,6]. In projection-diffusion

* Corresponding author.
E-mail address: boronski@gmail.com (P. Boronski).

0021-9991/$ - see front matter © 2007 Elsevier Inc. All rights reserved.
doi:10.1016/j.jcp.2007.08.023

schemes, approximate boundary conditions are imposed for the pressure [7]. For magnetic fields, however, the exact evolution of the equations conserves divergence and there exists no analogue to the pressure. Thus if the numerical algorithm creates divergence, there is no mechanism for eliminating it and it may accumulate [8]. For this reason, magnetohydrodynamic codes sometimes include a fictitious term analogous to the hydrodynamic pressure, which must be treated numerically [9]. Various methods for imposing a solenoidal magnetic field are compared in [10].

The second approach, which is the focus of this paper, is to express fields in such a way that they are divergence-free by construction. It can be proved that a field $\mathbf{F}$ which is solenoidal (divergence-free) in a simply connected domain can be written as:

$$\mathbf{F} = \nabla \times (\psi \hat{\mathbf{e}}) + \nabla \times \nabla \times (\phi \hat{\mathbf{e}}) \tag{1.1}$$

where $\hat{\mathbf{e}}$ denotes a unit vector. In addition to being divergence-free, $\mathbf{F}$ has the advantage of involving only two scalar fields. This makes more economical use of computer memory and allows all calculations to be implemented using only scalar fields.

Equations governing the evolution of the two potentials are derived by taking the curl and double curl of the original equations, increasing the order of the differential equations. In addition, boundary conditions, some also of high order, couple the two potentials. In most geometries with one nonperiodic direction, these are only minor obstacles [1]. In spectral treatments of such geometries, the basis functions insure periodicity, which is preserved under differentiation and addition. At most, special consideration must be given to constant modes. The standard examples are a spherical geometry [11–16] or a three-dimensional Cartesian geometry with one bounded direction and two perpendicular periodic directions, such as channel flow [17,18]. Other applications are in a cylindrical geometry with periodic z and θ directions [1,19,20].

In geometries with more than one nonperiodic direction, far more care is required. Marques [1] gave a detailed analysis of the poloidal–toroidal decomposition for the Navier–Stokes equations and its formulation and validity for general topologies. This analysis was then put into practice in a linear stability analysis of Rayleigh–Bénard convection in a finite cylindrical geometry [2]. However, the governing equations derived in [2] contain large linear systems that couple the potentials and their Laplacians and bilaplacians, but whose solution would be required in implicit time integration. Analogous problems arise in the other formulations of incompressible fluid dynamics. In the 2D streamfunction–vorticity formulation, the equations for the vorticity and the streamfunction are coupled by the fact that boundary conditions exist only for the streamfunction and none for the vorticity. In the $(\mathbf{u}, p)$ primitive variable formulation, the pressure is the solution to a Poisson problem for which the appropriate boundary condition is that the velocity be divergence-free [3,4].

Our primary goal in this paper is to demonstrate that the high-order equations can be separated via the influence matrix technique into a sequence of problems of lower order, each with its own boundary conditions, as was done for the primitive variable formulation in [3]. This makes implicit time integration feasible for the poloidal–toroidal decomposition in geometries with two nonperiodic directions. A secondary goal is to carry out the same analysis for a magnetic field which is governed by the induction equation and which generalizes the Navier–Stokes equation by the inclusion of the Lorentz force.

The equations we will consider are the magnetohydrodynamic equations:

$$\partial_t \mathbf{u} + (\mathbf{u} \cdot \nabla)\mathbf{u} = (\mathbf{B} \cdot \nabla)\mathbf{B} + Re^{-1} \Delta \mathbf{u} - \nabla \left(p + \frac{B^2}{2} \right) \tag{1.2a}$$

$$\nabla \cdot \mathbf{u} = 0 \tag{1.2b}$$

$$\partial_t \mathbf{B} = \nabla \times (\mathbf{u} \times \mathbf{B}) + R_{\mathrm{m}}^{-1} \Delta \mathbf{B} \tag{1.3a}$$

$$\nabla \cdot \mathbf{B} = 0 \tag{1.3b}$$

where Re is the usual hydrodynamic Reynolds number and R_{m} the magnetic Reynolds number. Equations (1.2) and (1.3) are of different types: for a divergence-free magnetic field $\mathbf{B}$, all the terms of (1.3) have zero divergence as well, but this is not the case for (1.2).

The velocity and magnetic fields are to be calculated in a finite cylinder. We consider specifically the case in which the flow is driven by rotating upper and lower disks, although our method does not depend on this. For

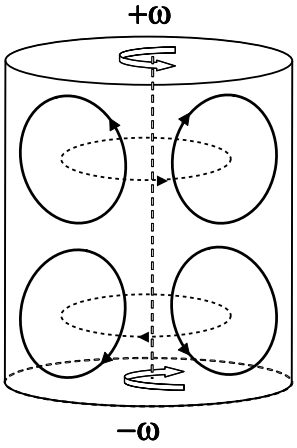

Fig. 1. Axisymmetric flow between counter-rotating disks. Poloidal component: solid curves. Toroidal component: dashed curves.

disks rotating in opposite directions this configuration is called the von Kármán flow [21–23]. The magnetic field inside the cylinder is required to match the field outside, which goes to zero at infinity. These boundary conditions are expressed as:

$$\mathbf{u} = 0 \qquad \text{at } r = 1, \tag{1.4a}$$

$$\mathbf{u} = r\omega_{\pm}\hat{\mathbf{e}}_{\theta} \qquad \text{at } z = \pm\frac{h}{2}, \tag{1.4b}$$

$$\mathbf{B}^{\text{int}} - \mathbf{B}^{\text{ext}} = 0 \qquad \text{on } \partial\Omega, \tag{1.5a}$$

$$\mathbf{B} = 0 \qquad \text{at infinity.} \tag{1.5b}$$

where Ω denotes the interior domain (the cylinder) and $\partial\Omega$ is its boundary. Although we will use equations (1.2) and (1.3) with boundary conditions (1.4) and (1.5) throughout this paper, the method may be formulated for other problems as well.

The poloidal and toroidal components for this configuration in the axisymmetric case with $\hat{\mathbf{e}} = \hat{\mathbf{e}}_z$ are illustrated in Fig. 1. The toroidal flow corresponds to motion with only azimuthal velocity. The poloidal flow forms recirculation rolls in the (r, z) plane. (This terminology comes from the spherical geometry, where the (r, z) flow travels from one pole to the other.) For a non-axisymmetric flow, there is no clear correspondence between each potential and a simple topological structure.

In Section 2, we give a general description of the poloidal–toroidal decomposition. In Section 3, we then specialize to the Navier–Stokes equations in a finite cylinder, formulating the boundary conditions for this case. In Section 4 we show how to decouple the equations and boundary conditions via the influence matrix technique. Finally, in Section 5, we present the equations and boundary conditions for the induction equation which governs the magnetic field, and the corresponding influence matrix.

2. Poloidal–toroidal decomposition

2.1. Governing equations

The poloidal–toroidal decomposition generalizes to three dimensions the two-dimensional streamfunction–vorticityy formulation. We follow the analysis and notation of [1], but specializing to the case of a domain which is contractible to a point (i.e. has no holes). Then:

$$\nabla \cdot \mathbf{F} = 0 \Longleftrightarrow \mathbf{F} = \nabla \times \mathbf{A} \tag{2.1}$$

A distinguished direction and associated unit vector $\hat{\mathbf{e}}$ is selected and $\mathbf{A}$ can be decomposed such that:

$$\mathbf{F} = \nabla \times \psi\hat{\mathbf{e}} + \nabla \times \nabla \times \phi\hat{\mathbf{e}} \tag{2.2}$$

The direction $\hat{\mathbf{e}}$ is called vertical and those perpendicular to $\hat{\mathbf{e}}$ are called horizontal; see Fig. 2. A number of possibilities exist for $\hat{\mathbf{e}}$. Among these, the choices $\hat{\mathbf{e}} = \hat{\mathbf{e}}_z$ (in Cartesian or cylindrical coordinates) or $\hat{\mathbf{e}} = \hat{\mathbf{e}}_\rho$ (the spherical radius) decouple ψ and ϕ in the diffusive operators since:

$$\hat{\mathbf{e}}\cdot\mathbf{F} = -\Delta_h\phi, \qquad \hat{\mathbf{e}}\cdot\Delta\mathbf{F} = -\Delta\Delta_h\phi, \tag{2.3a}$$

$$\hat{\mathbf{e}}\cdot\nabla\times\mathbf{F} = -\Delta_h\psi, \qquad \hat{\mathbf{e}}\cdot\nabla\times\Delta\mathbf{F} = -\Delta\Delta_h\psi, \tag{2.3b}$$

$$\hat{\mathbf{e}}\cdot\nabla\times\nabla\times\mathbf{F} = \Delta\Delta_h\phi, \quad \hat{\mathbf{e}}\cdot\nabla\times\nabla\times\Delta\mathbf{F} = \Delta\Delta\Delta_h\phi. \tag{2.3c}$$

where Δ_h is the two-dimensional Laplacian acting in the horizontal directions, i.e., those perpendicular to $\hat{\mathbf{e}}$. (The decoupling (2.3) does not hold [1] when the cylindrical radius $\hat{\mathbf{e}}_r$ is chosen as the distinguished direction $\hat{\mathbf{e}}$).

The equations for the velocity potentials are derived by taking the $\hat{\mathbf{e}}$ component of the single and double curl of (1.2); those for the magnetic potentials are derived by taking the $\hat{\mathbf{e}}$ component itself and the single curl of (1.3). The difference arises from the fact that all the terms of (1.3) are divergence-free and there is no pressure to eliminate. Combining (1.2), (1.3) and (2.3) leads to the evolution equations for the scalar potentials:

$$(\partial_t - \mathrm{Re}^{-1}\Delta)\Delta_h\psi_u = \hat{\mathbf{e}}\cdot\nabla\times\mathbf{S}_u \tag{2.4a}$$

$$(\partial_t - \mathrm{Re}^{-1}\Delta)\Delta\Delta_h\phi_u = -\hat{\mathbf{e}}\cdot\nabla\times\nabla\times\mathbf{S}_u \tag{2.4b}$$

$$(\partial_t - R_\mathrm{m}^{-1}\Delta)\Delta_h\phi_B = \hat{\mathbf{e}}\cdot\mathbf{S}_B \tag{2.5a}$$

$$(\partial_t - R_\mathrm{m}^{-1}\Delta)\Delta_h\psi_B = \hat{\mathbf{e}}\cdot\nabla\times\mathbf{S}_B \tag{2.5b}$$

where

$$\mathbf{S}_u \equiv (\mathbf{u}\cdot\nabla)\mathbf{u} - (\mathbf{B}\cdot\nabla)\mathbf{B} \tag{2.6a}$$

$$\mathbf{S}_B \equiv -\nabla\times(\mathbf{u}\times\mathbf{B}) \tag{2.6b}$$

Equations (2.4) and (2.5) are not all of the same order in the vertical and horizontal directions. For example, for the velocity, (2.4a) is second order in the vertical direction and fourth order in the horizontal directions, while (2.4b) is fourth order in the vertical direction and sixth order in the horizontal directions. A corresponding number of boundary conditions are required for the velocity potentials, a total of $(2+4)/2 = 3$ conditions at each vertical boundary and $(4+6)/2 = 5$ at each horizontal boundary for $\mathbf{u}$. The conditions at the vertical boundaries are those corresponding to the physical problem. At the horizontal boundaries, the physical conditions must be supplemented by two additional conditions whose derivation is the subject of the remainder of this section.

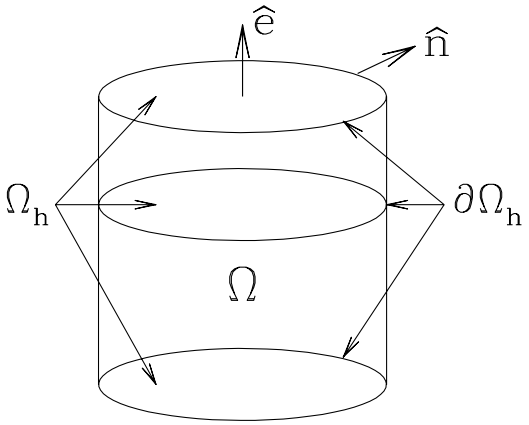

Fig. 2. Geometry for potential variable formulation. Ω is a cylindrical domain. The vector $\hat{\mathbf{e}}$ points in the distinguished vertical direction, here $\hat{\mathbf{e}}_z$. Ω_h are slices of Ω perpendicular to $\hat{\mathbf{e}}$, here disks. The boundary of Ω_h is $\partial\Omega_h$, here a circle. The vector $\hat{\mathbf{n}}$ is normal to both $\hat{\mathbf{e}}$ and to Ω_h; here $\hat{\mathbf{n}} = \hat{\mathbf{e}}_r$.

2.2. Gauge freedom

The poloidal–toroidal formulation (2.2) contains a gauge freedom for the choice of ψ and ϕ, which is identified by finding the class of potentials satisfying the homogeneous problem $\mathbf{F}=0$. For $\hat{\mathbf{e}}=\hat{\mathbf{e}}_z$ (Cartesian or cylindrical coordinate) or $\hat{\mathbf{e}}=\hat{\mathbf{e}}_\rho$ (spherical radius), this leads to:

$$\begin{aligned}
&\mathbf{F}^{\mathrm{hom}} = 0 = \nabla\times(\psi^{\mathrm{hom}}\hat{\mathbf{e}}) + \nabla\times\nabla\times(\phi^{\mathrm{hom}}\hat{\mathbf{e}})\\
&0 = \hat{\mathbf{e}}\times\nabla_h\psi^{\mathrm{hom}} + \nabla_h\partial_e\phi^{\mathrm{hom}} - (\Delta_h\phi^{\mathrm{hom}})\hat{\mathbf{e}}\\
&\qquad\qquad\Downarrow\\
&\hat{\mathbf{e}}\cdot\mathbf{F}^{\mathrm{hom}} = 0 \Rightarrow \Delta_h\phi^{\mathrm{hom}} = 0 \qquad (2.7a)\\
&\hat{\mathbf{e}}\times\mathbf{F}^{\mathrm{hom}} = 0 \Rightarrow \hat{\mathbf{e}}\times\nabla_h\psi^{\mathrm{hom}} = -\nabla_h\partial_e\phi^{\mathrm{hom}} \qquad (2.7b)
\end{aligned}$$

where e denotes the coordinate corresponding to $\hat{\mathbf{e}}$. The existence of ψ^{hom} satisfying (2.7b) for all ϕ^{hom} satisfying (2.7a) is demonstrated as follows. Condition (2.7a) implies:

$$\nabla_h\cdot(\nabla_h\partial_e\phi^{\mathrm{hom}}) = 0 \qquad (2.8)$$

Applying (2.1) to the simply connected two-dimensional domain slices perpendicular to $\hat{\mathbf{e}}$, (2.8) implies that there exists a ψ^{hom} satisfying:

$$\nabla_h\partial_e\phi^{\mathrm{hom}} = \nabla_h\times(-\psi^{\mathrm{hom}}\hat{\mathbf{e}}) = \hat{\mathbf{e}}\times\nabla_h\psi^{\mathrm{hom}} \qquad (2.9)$$

Thus, the poloidal potential ϕ is determined up to a harmonic function on each domain slice perpendicular to $\hat{\mathbf{e}}$:

$$\phi\sim\phi+\phi^{\mathrm{hom}};\quad \Delta_h\phi^{\mathrm{hom}}=0 \qquad (2.10a)$$

while ψ is determined up to an arbitrary function of the coordinate e:

$$\psi\sim\psi+h(e) \qquad (2.10b)$$

The choice of gauge constitutes one of the two additional conditions required.

2.3. Compatibility condition

We have not yet demonstrated the equivalence between the potential and primitive variable formulations. Since the curl of equations (1.2) and (1.3) were taken, they gained an additional degree of freedom which must be fixed in such a way that these equations in potential form (2.4) and (2.5) define the same velocity $\mathbf{u}$ and magnetic field $\mathbf{B}$ as the original MHD equations (1.2) and (1.3). We will require the fact that on a simply connected domain, a field is a gradient if and only if it is curl-free:

$$\mathbf{f}=\nabla p \Longleftrightarrow \nabla\times\mathbf{f}=0 \qquad (2.11)$$

which is a consequence of Stokes' theorem. We will first write (1.2) and (1.3) in a compact form, which will let us use a common form for (2.4) and (2.5):

$$\begin{aligned}
&\mathbf{f}_u \equiv (\partial_t - R\mathrm{e}^{-1}\Delta)\mathbf{u} + \mathbf{S}_u = -\nabla(p+B^2/2) \qquad (2.12a)\\
&\mathbf{g}_u \equiv \nabla\times\mathbf{f}_u = 0 \qquad (2.12b)\\
&\mathbf{g}_B \equiv (\partial_t - R_{\mathrm{m}}^{-1}\Delta)\mathbf{B} + \mathbf{S}_B = 0 \qquad (2.12c)
\end{aligned}$$

where (2.12a) and (2.12b) are equivalent, by (2.11). Then we can write the primitive variable formulation (1.2) and (1.3) and potential formulation (2.4) and (2.5) using for either $\mathbf{g}=\mathbf{g}_u$ or $\mathbf{g}=\mathbf{g}_B$:

$$\begin{array}{ll} \text{Primitive variables} & \text{Potential formulation}\\ \mathbf{g}=0 & \Rightarrow \begin{cases}\hat{\mathbf{e}}\cdot\mathbf{g}=0\\ \hat{\mathbf{e}}\cdot\nabla\times\mathbf{g}=0\end{cases}\end{array} \qquad (2.13)$$

Marques [1] proves that in a simply connected domain Ω, the potential and primitive variable formulations are equivalent if additional conditions are satisfied:

$$\mathbf{g} = 0 \Longleftrightarrow \begin{cases} \hat{\mathbf{e}} \cdot \mathbf{g} = 0 & \text{in } \Omega \quad \text{(a)} \\ \hat{\mathbf{e}} \cdot \nabla \times \mathbf{g} = 0 & \text{in } \Omega \quad \text{(b)} \\ \nabla \cdot \mathbf{g} = 0 & \text{in } \Omega \quad \text{(c)} \\ \hat{\mathbf{n}} \cdot \mathbf{g} = 0 & \text{on } \partial\Omega_h \quad \text{(d)} \end{cases} \tag{2.14}$$

In (2.14d), $\hat{\mathbf{n}}$ is the vector normal to the boundary $\partial\Omega_h$ of slices perpendicular to $\hat{\mathbf{e}}$. We recall that in our case, $\hat{\mathbf{e}} = \hat{\mathbf{e}}_z$, the slices Ω_h are disks, their boundaries $\partial\Omega_h$ are circles, and $\hat{\mathbf{n}} = \hat{\mathbf{e}}_r$ is the radial unit vector. We illustrate this geometry in Fig. 2.

The rightwards implication of (2.14) is obvious. The leftwards implication of (2.14) is proved as follows. We first use (2.14a) and the two-dimensional Stokes' Theorem (2.11) to introduce a scalar function κ

$$\left.\begin{aligned} 0 &= \hat{\mathbf{e}} \cdot \mathbf{g} \\ 0 &= \hat{\mathbf{e}} \cdot \nabla \times \mathbf{g} \end{aligned}\right\} \Rightarrow \mathbf{g} = \nabla_h \kappa \tag{2.15}$$

recalling that the subscript h restricts differential operators to the directions perpendicular to $\hat{\mathbf{e}}$; in our case the (r,θ) directions. We then use the additional divergence-free condition (2.14c) to show that κ is harmonic:

$$\left.\begin{aligned} \mathbf{g} &= \nabla_h \kappa \\ \nabla \cdot \mathbf{g} &= 0 \end{aligned}\right\} \Rightarrow \Delta_h \kappa = 0 \tag{2.16}$$

The additional condition (2.14d) then provides a Neumann boundary condition on κ:

$$\left.\begin{aligned} \Delta_h \kappa &= 0 \\ \hat{\mathbf{n}} \cdot \nabla \kappa &= 0 \quad \text{on } \partial\Omega_h \end{aligned}\right\} \Rightarrow \kappa = \kappa_0(e) \tag{2.17}$$

(see Fig. 2, where $e = z$). Finally

$$\mathbf{g} = \nabla_h \kappa(e) = 0 \tag{2.18}$$

since the ∇_h measures variation in the horizontal directions, which are perpendicular to the coordinate e. The divergence-free condition (2.14c) is satisfied for $\mathbf{u}$ since (2.12b) defines $\mathbf{g}_u$ as a curl. It is satisfied for $\mathbf{B}$ because (2.6) is divergence-free if $\mathbf{B}$ is, e.g. if $\mathbf{B}$ is expanded as (2.2).

Condition (2.14d), which is called the compatibility condition and which ensures the equivalence of both formulations, is the projection of the original equations normal to the boundary. Its interpretation is quite intuitive: the compatibility condition preserves information about the original equations which has been lost by taking the curl. This procedure is familiar from simpler contexts: when an equation is differentiated, it must be supplemented by a constant of integration, which is the evaluation of the original equation at a point. Condition (2.14d) is sufficient but not unique – other boundary conditions ensuring (2.14) exist.

We can extend the equivalence (2.14) proved in [1] to justify the transformed boundary conditions often used in practice in the toroidal–poloidal formulation. To impose the boundary condition $\mathbf{u} - \mathbf{u}^{\mathrm{bc}} = 0$ on a simply connected boundary $\partial\Omega$ with normal $\hat{\mathbf{e}}$, we substitute for the three vector components the conditions:

$$\hat{\mathbf{e}} \cdot (\mathbf{u} - \mathbf{u}^{\mathrm{bc}}) = 0 \qquad \text{on } \partial\Omega \tag{2.19a}$$

$$\hat{\mathbf{e}} \cdot \nabla \times (\mathbf{u} - \mathbf{u}^{\mathrm{bc}}) = 0 \quad \text{on } \partial\Omega \tag{2.19b}$$

$$\nabla_h \cdot (\mathbf{u} - \mathbf{u}^{\mathrm{bc}}) = 0 \qquad \text{on } \partial\Omega \tag{2.19c}$$

$$\hat{\mathbf{n}} \cdot (\mathbf{u} - \mathbf{u}^{\mathrm{bc}}) = 0 \qquad \text{on } \quad \partial(\partial\Omega) \tag{2.19d}$$

where $\partial(\partial\Omega)$ is the one-dimensional boundary of $\partial\Omega$ and $\hat{\mathbf{n}}$ is perpendicular both to this boundary and to $\hat{\mathbf{e}}$. Equation (2.19c) can be replaced by

$$\nabla \cdot [(\hat{\mathbf{e}} \cdot \mathbf{u})\hat{\mathbf{e}}] = \nabla \cdot \mathbf{u} - \nabla_h \cdot \mathbf{u}^{\mathrm{bc}} = 0 \quad \text{on } \partial\Omega \tag{2.19c$'$}$$

where the second equality is valid when $\mathbf{u}$ is divergence-free and the boundary conditions are homogeneous.

The transformed boundary conditions (2.19) are familiar in the context of a spherical or infinite planar surface, where the additional condition (2.19d) is not needed since these surfaces have no boundaries. For example, in the case of flow between two stationary infinite planes at $z = \pm 1$, boundary conditions (2.19) take the form:

$$w = 0 \quad \text{at } z = \pm 1 \tag{2.20a}$$
$$\eta = 0 \quad \text{at } z = \pm 1 \tag{2.20b}$$
$$\partial_z w = 0 \quad \text{at } z = \pm 1 \tag{2.20c}$$

where w and η are the vertical velocity and vorticity.

The derivation of both the gauge and the compatibility conditions depend on properties of the horizontal Laplace equation; see (2.10a) and (2.17). If the only harmonic function is a constant, the Neumann condition in (2.17) is superfluous. This is the case, for example, on the surface of a sphere. All horizontal directions are periodic, so that functions which grow monotonically in these directions are excluded; the compatibility condition (2.14d) can simply be dropped. However, in domains with more complicated topologies, such as those bounded by two infinite planes or cylinders considered to be doubly periodic, additional conditions are necessary in order for (2.11) to hold. A derivation of these conditions for a general domain can be found in [1].

3. Conditions on the velocity field

We now turn to the conditions to be imposed on the velocity field in the finite-cylindrical geometry for which $\hat{\mathbf{e}} = \hat{\mathbf{e}}_z$; see [2]. Because the next two sections will refer exclusively to the velocity, we drop the subscript u. For reference, we write for $\mathbf{F}$ defined in (2.2) the identities:

$$\mathbf{F} = -\hat{\mathbf{e}}_z \times \nabla_h \psi + \nabla_h \partial_z \phi - \hat{\mathbf{e}}_z \Delta_h \phi \tag{3.1a}$$
$$\nabla \times \mathbf{F} = -\hat{\mathbf{e}}_z \times \nabla_h \Delta \phi + \nabla_h \partial_z \psi - \hat{\mathbf{e}}_z \Delta_h \psi \tag{3.1b}$$
$$\Delta \mathbf{F} = -\hat{\mathbf{e}}_z \times \nabla_h \Delta \psi + \nabla_h \partial_z \Delta \phi - \hat{\mathbf{e}}_z \Delta_h \Delta \phi \tag{3.1c}$$
$$\nabla \times \Delta \mathbf{F} = \hat{\mathbf{e}}_z \times \nabla_h \Delta \Delta \phi + \nabla_h \partial_z \Delta \psi - \hat{\mathbf{e}}_z \Delta_h \Delta \psi \tag{3.1d}$$

which will facilitate calculations of vector quantities.

3.1. Gauge and boundary conditions

The governing equations are:

$$(\partial_t - \mathrm{Re}^{-1} \Delta) \Delta_h \psi = \hat{\mathbf{e}}_z \cdot \nabla \times \mathbf{S} \tag{3.2a}$$
$$(\partial_t - \mathrm{Re}^{-1} \Delta) \Delta \Delta_h \phi = -\hat{\mathbf{e}}_z \cdot \nabla \times \nabla \times \mathbf{S} \tag{3.2b}$$

The system (3.2) contains five Laplacians acting in the horizontal directions and three acting in the vertical directions. Three conditions in each direction are derived from the velocity boundary conditions. The two remaining conditions in the horizontal direction are the gauge and compatibility conditions.

The simplest choice of gauge is:

$$\phi = 0 \quad \text{at } r = 1 \tag{3.3a}$$

along with

$$\psi = 0 \quad \text{at } r = 0 \tag{3.3b}$$

On the cylinder, boundary conditions are imposed on u_r, u_θ, u_z. Referring to (3.1a), we have:

$$u_r = \frac{1}{r} \partial_\theta \psi + \partial_{rz} \phi = 0 \quad \text{at } r = 1 \tag{3.4a}$$
$$u_\theta = -\partial_r \psi + \frac{1}{r} \partial_{\theta z} \phi = 0 \quad \text{at } r = 1 \tag{3.4b}$$
$$u_z = -\Delta_h \phi = 0 \quad \text{at } r = 1 \tag{3.4c}$$

The gauge condition (3.3a) can be used to simplify (3.3b):

$$\phi = 0 \quad \Rightarrow \quad \partial_\theta \phi = \partial_z \phi = 0 \quad \Rightarrow \quad \partial_r \psi = 0 \quad \text{at } r = 1 \tag{3.4b'}$$

On the (simply connected) disks, we impose the boundary conditions in the form (2.19), i.e.

$$0 = u_z = -\Delta_h \phi \qquad \text{at } z = \pm\frac{h}{2} \tag{3.5a}$$

$$0 = \hat{\mathbf{e}}_z \cdot \nabla \times \mathbf{u} = -\Delta_h \psi - \frac{1}{r}\partial_r(r^2 \omega_\pm) \quad \text{at } z = \pm\frac{h}{2} \tag{3.5b}$$

$$0 = \partial_z u_z = -\partial_z \Delta_h \phi \qquad \text{at } z = \pm\frac{h}{2} \tag{3.5c}$$

These are equivalent to those on the individual components but easier to implement since each of (3.5) involves only one of the potentials. The remaining condition (2.19d) required on the two circles is insured by (3.4a).

3.2. Compatibility condition

We now turn to the compatibility condition (2.14d) for the hydrodynamic problem in our potential formulation, where $\hat{\mathbf{e}} \equiv \hat{\mathbf{e}}_z$, $\hat{\mathbf{n}} \equiv \hat{\mathbf{e}}_r$, and $\partial\Omega_h$ is the $r = 1$ boundary:

$$0 = \hat{\mathbf{e}}_r \cdot \mathbf{g} = \hat{\mathbf{e}}_r \cdot \nabla \times \mathbf{f} = \hat{\mathbf{e}}_r \cdot \nabla \times ((\partial_t - Re^{-1}\Delta)\mathbf{u} + \mathbf{S}) \quad \text{at } r = 1 \tag{3.6}$$

Because $\hat{\mathbf{e}}_r \cdot \nabla\times$ involves only ∂_θ and ∂_z, derivatives parallel to the $r = 1$ boundary, it vanishes for all terms in $\mathbf{f}$ which are zero or constant at this boundary. For homogeneous boundary conditions (3.4) on the outer cylinder, this is true for $\partial_t \mathbf{u}$ and for $\mathbf{S}$ defined in (2.6b) in the absence of a magnetic field, leaving only the Laplacian term. Referring to (3.1d), we have

$$\hat{\mathbf{e}}_r \cdot \nabla \times \Delta\mathbf{u} = \partial_{rz}\Delta\psi - \frac{1}{r}\partial_\theta \Delta\Delta\phi \tag{3.7}$$

Conditions (3.3a), (3.4c) and (3.5) allow the replacement of $\Delta\psi$ and $\Delta\phi$ at $r = 1$ by $\Delta_h\psi$ and $\Delta_h\phi$, which already appear in the governing equations (3.2), leading to

$$0 = \partial_{rz}\Delta_h\psi - \frac{1}{r}\partial_\theta \Delta\Delta_h\phi \quad \text{at } r = 1 \tag{3.8}$$

The complete set of conditions to be imposed on the velocity is then:

$$\frac{1}{r}\partial_\theta\psi + \partial_{rz}\phi = 0 \qquad \text{at } r = 1 \tag{3.9a}$$

$$\partial_r\psi = 0 \qquad \text{at } r = 1 \tag{3.9b}$$

$$\Delta_h\theta = 0 \qquad \text{at } r = 1 \tag{3.9c}$$

$$\phi = 0 \qquad \text{at } r = 1 \tag{3.9d}$$

$$\text{nonaxi: } \partial_{rz}\Delta_h\psi - \frac{1}{r}\partial_\theta\Delta\Delta_h\phi = 0 \qquad \text{at } r = 1 \tag{3.9e}$$

$$\text{axi: } \psi = 0 \qquad \text{at } r = 0 \tag{3.9f}$$

$$\Delta_h\psi = -\frac{1}{r}\partial_r(\omega_\pm r^2) \qquad \text{at } z = \pm\frac{h}{2} \tag{3.10a}$$

$$\partial_z\Delta_h\phi = 0 \qquad \text{at } z = \pm\frac{h}{2} \tag{3.10b}$$

$$\Delta_h\phi = 0 \qquad \text{at } z = \pm\frac{h}{2} \tag{3.10c}$$

These conditions are imposed on ϕ and ψ via the influence matrix method, as will be explained in Section 4.

In equations (3.9), we have marked conditions (3.9d) and (3.9e) as applying only to axisymmetric or to non-axisymmetric modes. This will be explained in the following section.

3.3. Spatial discretization and symmetry

We use the spectral spatial discretization:

$$f(r,\theta,z)=\sum_{m=-\left\lfloor\frac{M}{2}\right\rfloor}^{\left\lfloor\frac{M}{2}\right\rfloor} f^m(r,z)\mathrm{e}^{\mathrm{i}m\theta}=\sum_{m=-\left\lfloor\frac{M}{2}\right\rfloor}^{\left\lfloor\frac{M}{2}\right\rfloor}\sum_{k=0}^{K-1}\sum_{\substack{n=|m|\\ n+m\text{even}}}^{2N-1} f_{kn}^m\mathcal{Q}_n^m(r)\mathcal{T}_k\left(\frac{2z}{h}\right)\mathrm{e}^{\mathrm{i}m\theta} \tag{3.11}$$

and similarly for ϕ. The basis functions in the axial direction z are the standard Chebyshev polynomials $\mathcal{T}_k(2z/h)$. Those in the radial direction r are the non-standard polynomial basis $\mathcal{Q}_n^m(r)$ developed by Matsushima and Marcus [25]. Their principal property is that $\mathcal{Q}_n^m(r)\sim r^m$ as $r\to 0$, insuring their regularity at the origin. The basis functions in the azimuthal direction θ are the Fourier modes $\mathrm{e}^{\mathrm{i}m\theta}$. In (3.11), we do not introduce new notation for Fourier coefficients, or for coefficients in the 3D tensor-product basis, instead distinguishing between physical space values and spectral space coefficients by the number and type of superscripts and subscripts.

The decomposition (3.11) leads to problems and boundary conditions which are decoupled for each Fourier wavenumber m. In fact, because of the reflection symmetry in z, the problems can be further reduced. A vector field is reflection-symmetric in z if u_r, u_θ are even in z and u_z is odd in z, i.e. if the potential ψ is even in z and the potential ϕ is odd in z, as can be seen from (3.1). We denote these functions as having parity $p=s$. Quantities related to anti-reflection-symmetric vector fields, i.e. with ψ odd and ϕ even, will be denoted as having parity $p=a$. The boundary conditions (3.9) at $r=1$ can be considered as applying separately to fields of each parity; note that (3.9a) and (3.9e) couple potentials of the same parity. The conditions (3.10) at $z=\pm h/2$ can be reformulated to apply only to fields of a single parity; for example $\Delta_h\phi(z=\pm\frac{h}{2})=0$ can be rewritten as $\Delta_h\phi(z=h/2)\pm\Delta_h\phi(z=-h/2)=0$. Essentially, a problem posed over the entire cylinder can be viewed as $2(M+1)$ problems in the two-dimensional meridional half-slice $0\leqslant r\leqslant 1$, $0\leqslant z\leqslant h/2$.

Special conditions are applied to the axisymmetric modes. The gauge freedom (2.10b) for ψ requires the specification of a single value of ψ at each z. In (3.9f), we have chosen to specify this value at the origin:

$$\psi(r=0,\theta,z)=\sum_m \psi^m(r=0,z)\mathrm{e}^{\mathrm{i}m\theta}=\psi^{m=0}(0,z) \tag{3.12}$$

Condition (3.9f) is applied only to the axisymmetric mode, since only this mode contributes to the sum (3.12).

For the axisymmetric modes, two important consequences are derived from the calculation for an arbitrary function $f^{m=0}(r)$

$$(r\partial_r f^0)(r=R)=r\partial_r f^0\big|_{r=0}^{r=R}=\int_0^R \mathrm{d}r\partial_r r\partial_r f^0=\int_0^R r\,\mathrm{d}r\frac{1}{r}\partial_r r\partial_r f^0=\int_0^R r\,\mathrm{d}r\Delta_h f^0 \tag{3.13}$$

Going from left to right in (3.13), one obtains the classic solvability condition required by Neumann boundary conditions, since setting the value of $\partial_r f^0(r=R)$ is equivalent to an integral constraint on $\Delta_h f^0$. In particular, the Neumann boundary condition (3.9b) on ψ must be replaced by the integral constraint like (3.13) for the axisymmetric mode. Going from right to left in (3.13) leads to the conclusion that the only axisymmetric harmonic function on a disk that includes the origin is a constant, since $\Delta_h f^0=0$ over $[0,R]$ implies $\partial_r f^0(r=R)=0$ for each R. This implies that the Neumann boundary condition in (2.17) is unnecessary to guarantee $\mathbf{g}=0$ for the axisymmetric mode, and hence that the compatibility condition (3.9e) should not be imposed on the axisymmetric mode.

Corresponding to the removal of the compatibility condition, Marques [1] showed that the system of equations governing the axisymmetric modes is of lower order. The calculation

$$\partial_r^+ f^0\equiv\frac{1}{r}\partial_r r f^0=0\Rightarrow f^0=\frac{c}{r}\Rightarrow f^0=0 \tag{3.14}$$

demonstrates the invertibility of ∂_r^+, or equivalently, the impossibility on a disk of a non-zero divergence-free axisymmetric radial vector field which is regular at the origin. Using (3.14), equations (2.4) and (2.5) become PDEs of lower order in $\partial_r\psi^0$ and $\partial_r\phi^0$:

$$(\partial_t - Re^{-1}\Delta^+)\partial_r\psi_u^0 = \hat{\mathbf{e}}_\theta \cdot \mathbf{S}_u^0 \tag{3.15a}$$

$$(\partial_t - Re^{-1}\Delta^+)\Delta^+\partial_r\phi_u^0 = -\hat{\mathbf{e}}_\theta \cdot (\nabla \times \mathbf{S}_u^0) \tag{3.15b}$$

$$(\partial_t - R_m^{-1}\Delta^+)\partial_r\phi_B^0 = \hat{\mathbf{e}}_\theta \cdot \mathbf{S}_B^0 \tag{3.15c}$$

$$(\partial_t - R_m^{-1}\Delta^+)\partial_r\psi_B^0 = \hat{\mathbf{e}}_\theta \cdot \nabla \times \mathbf{S}_B^0 \tag{3.15d}$$

where $\Delta^+ \equiv \partial_r\partial_r^+ + \partial_z^2$. In the interests of uniformity we continue to solve the same equations for the axisymmetric as for the non-axisymmetric modes, altering only the boundary conditions.

4. Nested Helmholtz and Poisson solvers

4.1. Temporal discretization

We briefly mention some aspects of our temporal discretization. A more extensive description of both the temporal and the spatial discretization is given in [24,26]. We recall the equations governing the velocity potentials:

$$(\partial_t - Re^{-1}\Delta)\Delta_h\psi = \hat{\mathbf{e}}_z \cdot \nabla \times \mathbf{S} \equiv S_\psi \tag{4.1a}$$

$$(\partial_t - Re^{-1}\Delta)\Delta\Delta_h\phi = -\hat{\mathbf{e}}_z \cdot \nabla \times \nabla \times \mathbf{S} \equiv S_\phi \tag{4.1b}$$

Evolution equations such as (4.1) are typically discretized in time via an implicit scheme for the diffusive terms and an explicit scheme for the nonlinear terms. For example, with the simplest choice of the backwards and forwards first-order Euler formulas, the diffusion equation

$$(\partial_t - Re^{-1}\Delta)f = S \tag{4.2a}$$

becomes

$$\frac{f(t+\delta t) - f(t)}{\delta t} - Re^{-1}\Delta f(t+\delta t) = S(t)$$

$$\left(I - \frac{\delta t}{Re}\Delta\right) f(t+\delta t) = f(t) + \delta t S(t) \tag{4.2b}$$

Thus implicit-diffusive/explicit-nonlinear temporal discretization transforms the parabolic equation (4.2a) into the Helmholtz problem (4.2b) for $f(t+\delta t)$. Similarly, the temporally discretized versions of the more complicated equations (4.1) give $\psi(t+\delta t)$ and $\phi(t+\delta t)$ as solutions to a sequence of nested Helmholtz and Poisson problems. This formulation can also be adapted to higher-order temporal schemes; see [26]. We will not distinguish between the continuous-time parabolic operators of type (4.2a) and the discretized Helmholtz operators of type (4.2b) and refer to both as Helmholtz problems.

4.2. Substitution of Dirichlet boundary conditions

Equations (3.9) and (3.10) give the set of boundary conditions which is to be imposed on (4.1). The major difficulty of the poloidal–toroidal formulation is that set (3.9) and (3.10), while appropriate for the entire problem, does not provide separate boundary conditions appropriate to each individual Helmholtz and Poisson problem. Some of the conditions involve both ψ and ϕ. Even conditions involving only one potential can be problematic because the order of the equations and of the boundary conditions do not match. The prototypical example of this occurs in the 2D streamfunction–vorticity formulation. At each timestep, one would like to solve successively the Helmholtz problem for the vorticity, and the Poisson problem for the streamfunction. However, no boundary conditions are available for the vorticity, while the streamfunction must satisfy both Dirichlet and Neumann boundary conditions.

The influence matrix technique [3,5,6] calls for replacing the problematic boundary conditions by conditions which are easier to implement numerically, in this case Dirichlet boundary conditions on a set of intermediate fields. The values used in these boundary conditions are determined in such a way that the exact

boundary conditions are satisfied. We show below the sequence of problems with their associated boundary conditions:

$$(\partial_t - Re^{-1}\Delta) f_\psi = S_\psi \tag{4.3a}$$

$$f_\psi = -\frac{1}{r}\partial_r(r^2\omega_\pm) \qquad \text{at } z = \pm\frac{h}{2} \tag{4.3b}$$

$$\text{axi:} \quad \int_0^r r dr f_\psi = 0 \qquad \text{at } r = 1 \tag{4.3c}$$

$$\begin{aligned} \text{nonaxi:} \quad & f_\psi = \sigma_f(z) \quad \text{at } r = 1 \\ & \Uparrow \\ & c_f(z) \equiv \left(\partial_{rz} f_\psi - \tfrac{1}{r}\partial_\theta g_\phi\right)\big|_{r=1} = 0 \end{aligned} \tag{4.3d}$$

$$\Delta_h \psi = f_\psi \tag{4.3e}$$

$$\text{axi:} \quad \psi = 0 \qquad \text{at } r = 0 \tag{4.3f}$$

$$\text{nonaxi:} \quad \partial_r \psi = 0 \qquad \text{at } r = 1 \tag{4.3g}$$

$$(\partial_t - Re^{-1}\Delta) g_\phi = S_\phi \tag{4.3h}$$

$$\begin{aligned} & g_\phi = \sigma_g^\pm(r) \qquad \text{at } z = \pm\tfrac{h}{2} \\ & \Uparrow \\ & c_g^\pm(r) \equiv \partial_z f_\phi\big|_{z=\pm\frac{h}{2}} = 0 \end{aligned} \tag{4.3i}$$

$$\begin{aligned} & g_\phi = \sigma_g(z) \qquad \text{at } r = 1 \\ & \Uparrow \\ & c_g(z) \equiv \left(\tfrac{1}{r}\partial_\theta \psi + \partial_{rz}\phi\right)\big|_{r=1} = 0 \end{aligned} \tag{4.3j}$$

$$\Delta f_\phi = g_\phi \tag{4.3k}$$

$$f_\phi = 0 \qquad \text{at } r = 1 \tag{4.3l}$$

$$f_\phi = 0 \qquad \text{at } z = \pm\frac{h}{2} \tag{4.3m}$$

$$\Delta_h \phi = f_\phi \tag{4.3n}$$

$$\phi = 0 \qquad \text{at } r = 1 \tag{4.3o}$$

We have introduced intermediate variables f_ψ, g_ϕ and f_ϕ, and required them to obey Dirichlet boundary conditions with unknown values $\sigma_f(z)$, $\sigma_g(z)$ and $\sigma_g^\pm(r)$, or 0. We have also introduced the notation $c_f(z)$, $c_g(z)$, and $c_g^\pm(r)$ for quantities which should be zero if the actual boundary conditions were satisfied. The boundary conditions in (4.3) are identical to (3.9)–(3.10), restated where possible in terms of f_ψ, g_ϕ and f_ϕ. The influence matrix establishes the correspondence between $\{\sigma_f, \sigma_g, \sigma_g^\pm\}$ and $\{c_f, c_g, c_g^\pm\}$. No significance should be attached to the choice of equation in (4.3) at which each c is defined, i.e. the elliptic problem with which each of the original boundary conditions has been associated. The correspondence serves merely to establish that the number of unknown Dirichlet values σ is the same as the number of boundary conditions $c = 0$.

In order to simplify the notation, we have suppressed the indices labelling the azimuthal Fourier wavenumber m and axial parity $p \in \{s, a\}$. Each equation in (4.3) should in fact be interpreted as applying separately to modes with different (m, p) values. Wherever it occurs, ∂_θ should be interpreted as multiplication by im, while in equation (4.3b), the right-hand-side is axisymmetric and hence should be interpreted as zero for $m \neq 0$. Note that the boundary conditions for the axisymmetric and non-axisymmetric modes differ slightly, as explained in Section 3.3.

4.3. Influence matrix method

System (4.3) is solved by generalizing the standard decomposition of a linear boundary value problem into particular and homogeneous problems, in which the boundary conditions or right-hand-side are set to zero, respectively. Here, the nature of the boundary conditions and the intermediate solutions to which they are applied are also changed. Historically, the name capacitance matrix has also been used to denote what we call the influence matrix; this has guided our choice of notation $\mathcal{C}$. The steps for carrying out the influence matrix technique are as follows.

4.3.1. Preprocessing step (homogeneous solutions):

- We calculate solutions to the homogeneous problem ($\mathbf{S} = 0$) with a complete set of Dirichlet boundary conditions corresponding to the spectral discretization (3.11). Specifically, for each Fourier mode $m \in \{0, \ldots, \frac{M}{2}\}$ and axial parity $p \in \{s, a\}$, the boundary values $\{\sigma_f(z), \sigma_g(z), \sigma_g^{\pm}(r)\}$ are set successively to:

$$\left\{\sigma_f(z) = \mathcal{T}_k\left(\frac{2z}{h}\right), \quad \sigma_g(z) = 0, \quad \sigma_g^+(r) = 0, \quad \sigma_g^-(r) = 0\right\} \tag{4.4a}$$

$$\left\{\sigma_f(z) = 0, \quad \sigma_g(z) = \mathcal{T}_k\left(\frac{2z}{h}\right), \quad \sigma_g^+(r) = 0, \quad \sigma_g^-(r) = 0\right\} \tag{4.4b}$$

$$\left\{\sigma_f(z) = 0, \quad \sigma_g(z) = 0, \quad \sigma_g^+(r) = \mathcal{Q}_n^m(r), \quad \sigma_g^-(r) = \mathcal{Q}_n^m(r)\right\} \tag{4.4c}$$

$$\left\{\sigma_f(z) = 0, \quad \sigma_g(z) = 0, \quad \sigma_g^+(r) = \mathcal{Q}_n^m(r), \quad \sigma_g^-(r) = -\mathcal{Q}_n^m(r)\right\} \tag{4.4d}$$

- For each homogeneous solution, the values of the unsatisfied conditions c_f, c_g, $c_g^{\pm}$ are calculated on the boundary.
- These are collected to form the $2(M+1)$ influence matrices $\mathcal{C}^{mp}$, each of size $(K+N)\times(K+N)$. Each set of Dirichlet boundary values leads to one column of $\mathcal{C}^{mp}$.
- The influence matrices are inverted to form $(\mathcal{C}^{mp})^{-1}$. Difficulties and techniques related to this inversion are discussed in Appendix A.

4.3.2. Each timestep (particular and final solutions):

- We calculate the particular solution, i.e. the solution to the inhomogeneous problem ($\mathbf{S} \neq 0$) with homogeneous Dirichlet boundary conditions $\sigma_f = \sigma_g = \sigma_g^{\pm} = 0$.
- We calculate the values of the unsatisfied conditions $\{c_f, c_g, c_g^{\pm}\}$ on the boundary. These are separated according to Fourier mode m and axial parity p.
- Each set (m,p) of c values is multiplied by the corresponding matrix $(\mathcal{C}^{mp})^{-1}$ to obtain appropriate values of $\{\sigma_f, \sigma_g, \sigma_g^{\pm}\}$.
- The inhomogeneous problem is then solved again with corrected inhomogeneous Dirichlet boundary values.

Axial symmetry is taken into account by examining (4.3). For solutions which are reflection-symmetric in z ($p = s$), σ_f is even in z, i.e. k takes only even values in (4.4a), while σ_g is odd in z, so k takes only odd values in (4.4b). Additionally, only (4.4d) is used. The corresponding c_f is odd, and c_g, c_g^{pm} are even in z. The opposite holds for fields which are anti-reflection symmetric in z ($p = a$): k takes only odd values in (4.4a) and even values in (4.4b) and only (4.4c) is used.

This decomposition can be expressed mathematically as a version of the Sherman–Morrison–Woodbury formula [3]. Here, a large problem coupling f_ψ, ψ, g_ϕ, f_ϕ, ϕ is decoupled by a transformation (the change in boundary conditions) of low rank $(K+N)$. The solution to the coupled problem can be obtained from that of the decoupled problem using an additional multiplication by a matrix of dimension $K+N$.

5. Towards an MHD solver

We now address the solution of the induction equation in a finite cylinder of finite conductivity surrounded by a vacuum extending to infinity. For a sphere or axially infinite cylinder, the boundary between interior and exterior domains is associated only with the radial coordinate. The boundary surrounding a finite cylinder, however, is specified as a relation between r and z. One approach is to define the induction equation in an integral formulation. The most important advantage is that no boundary conditions must be specified. Using this formulation [27], a stationary kinematic dynamo problem was solved in a cylindrical geometry. In [28,29], a finite volume method is used to discretize the solution in the interior, which is matched to that in the exterior vacuum via a boundary element method. An integral equation formulation was applied to the entire domain in [30,31] uses finite elements with a penalty method to apply boundary conditions. To our knowledge, however, there exists as yet no method applicable to the spectral formulation in a finite cylinder.

5.1. Matching conditions and gauge

In the remainder of this section, fields or potentials without subscripts or superscripts will be taken to refer to the interior magnetic field, while fields or potentials relating to the field in the exterior vacuum will be designated by a superscript, e.g. $\mathbf{B}^{\mathrm{vac}}$, ϕ^{vac}. We recall the equations governing the interior magnetic potentials:

$$(\partial_t - R_{\mathrm{m}}^{-1}\Delta)\Delta_h\phi = \hat{\mathbf{e}}\cdot\mathbf{S} \equiv S_\phi \tag{5.1a}$$

$$(\partial_t - R_{\mathrm{m}}^{-1}\Delta)\Delta_h\psi = \hat{\mathbf{e}}\cdot\nabla\times\mathbf{S} \equiv S_\psi \tag{5.1b}$$

System (5.1) requires two boundary conditions at each bounding surface and supplementary gauge and compatibility conditions at the horizontal boundary. The exterior magnetic field in a vacuum is described by a single harmonic potential which requires one boundary condition at each bounding surface; see 5.2 Thus a total of three matching conditions must be applied at each bounding surface:

$$0 = (B_r - B_r^{\mathrm{vac}}) = \frac{1}{r}\partial_\theta\psi + \partial_r(\partial_z\phi - \phi^{\mathrm{vac}}) \qquad \text{on } \partial\Omega \tag{5.2a}$$

$$0 = (B_\theta - B_\theta^{\mathrm{vac}}) = -\partial_r\psi + \frac{1}{r}\partial_\theta(\partial_z\phi - \phi^{\mathrm{vac}}) \quad \text{on } \partial\Omega \tag{5.2b}$$

$$0 = (B_z - B_z^{\mathrm{vac}}) = -\Delta\phi + \partial_z(\partial_z\phi - \phi^{\mathrm{vac}}) \qquad \text{on } \partial\Omega \tag{5.2c}$$

On the bounding cylinder $r = 1$, equations (5.2b) and (5.2c) (but not (5.2a)) can be simplified by choosing the gauge:

$$0 = (\partial_z\phi - \phi^{\mathrm{vac}}) \quad \text{at } r = 1 \tag{5.3}$$

leading to:

$$0 = \frac{1}{r}\partial_\theta\psi + \partial_r(\partial_z\phi - \phi^{\mathrm{vac}}) \qquad \text{at } r = 1 \tag{5.4a}$$

$$0 = \partial_r\psi \qquad \text{at } r = 1 \tag{5.4b}$$

$$0 = \Delta\phi \qquad \text{at } r = 1 \tag{5.4c}$$

On the disks $z = \pm h/2$, we use the boundary condition (2.19b), which becomes:

$$0 = \hat{\mathbf{e}}_z\cdot\nabla\times(\mathbf{B} - \mathbf{B}^{\mathrm{vac}}) = -\Delta_h\psi \quad \text{at } z = \pm\frac{h}{2} \tag{5.5a}$$

since the exterior magnetic field is curl-free. Thus ψ is harmonic on the disks, with homogeneous Neumann boundary condition (5.4b) and is therefore constant on each disk. The matching conditions (5.2a) and

(5.2b) can be applied at the disks to show that $\partial_z\phi - \phi^{\text{vac}}$ is constant on each disk, while the gauge condition (5.3) shows that the constant is zero:

$$0 = \partial_z\phi - \phi^{\text{vac}} \quad \text{at } z = \pm\frac{h}{2} \tag{5.5b}$$

The matching conditions at $z = \pm\frac{h}{2}$ are completed by applying (5.2c) at the disks:

$$0 = -\Delta\phi + \partial_z(\partial_z\phi - \phi^{\text{vac}}) = -\Delta_h\phi - \partial_z\phi^{\text{vac}} \quad \text{at } z = \pm\frac{h}{2} \tag{5.5c}$$

The final set of gauge and matching conditions to be imposed is (5.3), (5.4) and (5.5).

5.2. Exterior magnetic field

Since the exterior magnetic field has both zero curl and zero divergence, and the exterior domain is simply connected, (2.11) states that the exterior magnetic field can be represented as:

$$\mathbf{B}^{\text{vac}} = \nabla\phi^{\text{vac}} \tag{5.6}$$

where ϕ^{vac} satisfies:

$$\Delta\phi^{\text{vac}} = 0 \quad \text{outside the cylinder} \tag{5.7a}$$

$$\nabla\phi^{\text{vac}} = 0 \quad \text{at infinity} \tag{5.7b}$$

Equation (5.7b) supplies the boundary condition on ϕ^{vac} at infinity, while conditions on the cylindrical boundary are provided by coupling with the interior potentials via the gauge and matching conditions 5.3, 5.4a, 5.4b and 5.5c.

Although (5.7) is posed in the infinite domain outside the cylinder, we can avoid discretizing the infinite domain and solving numerically by using known analytic solutions to the Laplace equation. Our approach is to formulate a complete set of analytic solutions to (5.7), each of whose derivatives can be calculated. The exterior solution ϕ^{vac} can be expanded in this set, with coefficients related to values on the cylindrical boundary. The normal derivatives at the boundary can then be evaluated in terms of these coefficients. This defines a correspondence between a set of boundary values $\{\phi^{\text{vac}}|_{\partial\Omega}\}$ and a set of normal derivatives $\{\hat{\mathbf{n}}\cdot\nabla\phi^{\text{vac}}|_{\partial\Omega}\}$. This correspondence, or influence matrix, constitutes a basis for the Dirichlet-to-Neumann mapping for the domain outside the finite cylinder. The normal derivatives appearing in the matching conditions (5.4a) and (5.5c) can then be replaced by functions $\mathcal{F}_r \equiv \partial_r\phi^{\text{vac}}|_{r=1}$ and $\mathcal{F}_z^{\pm} \equiv \partial_z\phi^{\text{vac}}|_{z=\pm\frac{h}{2}}$ of the boundary values $\{\phi^{\text{vac}}|_{\partial\Omega}\}$. Equations (5.3) and (5.5b) in turn relate the boundary values of the exterior and interior potentials via $\phi^{\text{vac}}|_{\partial\Omega} = \partial_z\phi|_{\partial\Omega}$. The exterior magnetic field no longer appears and the interior problem is closed. Essentially, we seek to replace the matching conditions (5.3), (5.5b), (5.4a), (5.5c) by:

$$0 = \frac{1}{r}\partial_\theta\psi + \partial_{rz}\phi - \mathcal{F}_r(\{\partial_z\phi|_{\partial\Omega}\}) \quad \text{at } r = 1 \tag{5.8a}$$

$$0 = -\Delta_h\phi - \mathcal{F}_z^{\pm}(\{\partial_z\phi|_{\partial\Omega}\}) \qquad \text{at } z = \pm\frac{h}{2} \tag{5.8b}$$

The task is now to obtain a well conditioned matrix representation of the Dirichlet-to-Neumann mappings $\mathcal{F}_r, \mathcal{F}_z^{\pm}$.

We have considered two sets of solutions to (5.7). The first set is constructed from the classic spherical harmonics. That is, we expand ϕ^{vac} as:

$$\begin{aligned}\phi^{\text{vac}} &= \phi_\infty^{\text{vac}} + \sum_m \sum_{l\geqslant|m|} \phi_{lm}^{\text{vac}}\rho^{-(l+1)}P_{lm}(\cos\xi)e^{im\theta} \\ \rho &= \sqrt{r^2+z^2}, \quad \xi = \tan^{-1}\left(\frac{r}{z}\right)\end{aligned} \tag{5.9}$$

where P_{lm} are the associated Legendre polynomials. According to (5.6), ϕ^{vac} is defined only up to a constant, which we may choose such as to set $\phi_\infty^{\text{vac}} = 0$. (In two dimensions, i.e. for a function whose gradient decays as the cylindrical radius r, rather than the spherical radius ρ, tends to infinity, logarithmic functions

would have to be included in the expansion because it cannot be assumed that ϕ^{vac} tends to a constant at infinity.) For a given longitudinal Fourier mode m, the solution (5.9) has degrees of freedom associated with index l, associated with the latitude. In the standard spectral–physical space duality, the set of coefficients ϕ^{vac}_{lm} corresponds to the set of values $\phi^{\mathrm{vac}}_{m}(r_i,z_i)$ for (r_i,z_i) on the boundary and can be determined from them by solving:

$$\begin{aligned}\phi^{\mathrm{vac}}_{m}(r_i,z_i) &= \sum_{l=|m|}^{|m|+L-1} \phi^{\mathrm{vac}}_{lm}\rho_i^{-(l+1)}P_{lm}(\cos\xi_i)\\ \rho_i &= \sqrt{r_i^2+z_i^2},\quad \xi_i = \tan^{-1}\left(\frac{r_i}{z_i}\right)\end{aligned} \tag{5.10}$$

where L is the number of points on the boundary. Expansion (5.9) readily yields the normal derivatives $\partial_r\phi^{\mathrm{vac}}_{m}(r_i,z_i), \partial_z\phi^{\mathrm{vac}}_{m}(r_i,z_i)$ at the boundary in terms of the coefficients ϕ^{vac}_{lm}. However, this approach is not feasible, in part because the transform (5.10) is extremely poorly conditioned, like all other transforms involving monomials. As l increases, the functions $\rho_i^{-(l+1)}$ become spiked at the largest values of ρ_i and zero elsewhere, a difficulty which does not arise on a spherical surface where ρ is constant.

We have also considered a second set of solutions to (5.7), constructed from the equally classic free-space or fundamental Green's functions:

$$\phi^{\mathrm{vac}}(\mathbf{x}) = \int_{\partial\Omega} \frac{\mathrm{d}\mathbf{x}'}{4\pi|\mathbf{x}-\mathbf{x}'|}\sigma(\mathbf{x}') \tag{5.11}$$

where $\sigma(\mathbf{x}')$ is a distribution on the cylindrical surface $\partial\Omega$ which is calculated in such a way as to yield a particular set of boundary values for $\phi^{\mathrm{vac}}(\mathbf{x})$ and $G(\mathbf{x},\mathbf{x}') = 4\pi/|\mathbf{x}-\mathbf{x}'|$ satisfies

$$\Delta'_{\mathbf{x}}G(\mathbf{x},\mathbf{x}') = \delta(\mathbf{x}-\mathbf{x}') \tag{5.12}$$

The derivatives of expansion (5.11) are obtained by differentiating the Green's functions:

$$\nabla_{\mathbf{x}}\phi^{\mathrm{vac}}(\mathbf{x}) = \int_{\partial\Omega} \mathrm{d}\mathbf{x}' \frac{\mathbf{x}-\mathbf{x}'}{4\pi|\mathbf{x}-\mathbf{x}'|^3}\sigma(\mathbf{x}') \tag{5.13}$$

This approach is discussed and shown to perform quite well for a two-dimensional test problem in [32]. The exterior fields generated approximate the solution uniformly near the boundary and converge exponentially with resolution; the influence matrix representing the Dirichlet-to-Neumann mapping is well conditioned.

5.3. Magnetic compatibility condition

The magnetic compatibility condition, obtained by substituting (2.12c) into (2.14d), is:

$$0 = \hat{\mathbf{e}}_r\cdot\mathbf{g}_B = \hat{\mathbf{e}}_r\cdot((\partial_t - R_{\mathrm{m}}^{-1}\Delta)\mathbf{B} + \mathbf{S}_B) \quad \text{at } r=1 \tag{5.14}$$

Contrary to the velocity, the magnetic field does not vanish on the boundary so $\partial_t\mathbf{B}\neq 0$. The nonlinear term $\mathbf{S}_B = \nabla\times(\mathbf{u}\times\mathbf{B})$ does vanish at the boundary since $\mathbf{u}|_{r=1}=0$ and its radial curl $\hat{\mathbf{e}}_r\cdot\mathbf{S}_B$ contains no normal derivatives of $\mathbf{u}$. The remaining terms are evaluated using (3.1a) and (3.1c):

$$0 = \hat{\mathbf{e}}_r\cdot(\partial_t - R_{\mathrm{m}}^{-1}\Delta)\mathbf{B} = \frac{1}{r}\partial_\theta(\partial_t - R_{\mathrm{m}}^{-1}\Delta)\psi + \partial_{rz}(\partial_t - R_{\mathrm{m}}^{-1}\Delta)\phi \quad \text{at } r=1 \tag{5.15}$$

The magnetic compatibility equation must use the same time discretization as the evolution equations, here backwards Euler. Although the the time derivative in (5.15) may seem difficult to include in an implementation of the influence matrix, the boundary operator in (5.15) can be decomposed into two parts, one which acts on the homogeneous solution at time $t+\delta t$ (and contributes to the influence matrix) and the other which acts on the particular solution at time $t+\delta t$ and the actual solution at time t. Details are given in [24].

The velocity compatibility condition (3.9e) must also be modified to include a contribution from the magnetic field:

$$0 = \partial_{rz}\Delta_h\psi_u - \frac{1}{r}\partial_\theta\Delta\Delta_h\phi_u - \hat{\mathbf{e}}_r\cdot\nabla\times(\mathbf{B}\cdot\nabla)\mathbf{B} \quad \text{at } r=1 \tag{5.16}$$

5.4. Nested elliptic problems and influence matrix

The set of nested Helmholtz and Poisson problems (5.1), together with the conditions (5.4b), (5.4c), (5.5a), (5.8) and (5.15) can be solved using the influence matrix technique, as was done for the velocity in Section 4.2 and in equation (4.3).

$$(\partial_t - \mathrm{Re}^{-1}\Delta)f = S_\psi \tag{5.17a}$$

$$f = 0 \qquad \text{at } z = \pm\frac{h}{2} \tag{5.17b}$$

$$\text{axi:}\quad \int_0^r r\,\mathrm{d}r f = 0 \qquad \text{at } r=1 \tag{5.17c}$$

$$\begin{aligned}\text{nonaxi:}\quad & f = \sigma_f(z) \qquad \text{at } r=1\\ & \Uparrow\\ & c_f(z) \equiv \left[\tfrac{1}{r}\partial_\theta(\partial_t - R_\mathrm{m}^{-1}\Delta)\psi + \partial_{rz}(\partial_t - R_\mathrm{m}^{-1}\Delta)\phi\right]\big|_{r=1} = 0\end{aligned} \tag{5.17d}$$

$$\Delta_h\psi = f \tag{5.17e}$$

$$\text{axi:}\quad \psi = 0 \qquad \text{at } r=0 \tag{5.17f}$$

$$\text{nonaxi:}\quad \partial_r\psi = 0 \qquad \text{at } r=1 \tag{5.17g}$$

$$(\partial_t - \mathrm{Re}^{-1}\Delta)g = S_\phi \tag{5.17h}$$

$$\begin{aligned}& g = \sigma_g(z) \qquad \text{at } r=1\\ & \Uparrow\\ & c_g(z) \equiv \Delta\phi|_{r=1} = 0\\ & g = \sigma_g^\pm(r) \qquad \text{at } z = \pm\tfrac{h}{2}\\ & \Uparrow\\ & c_g^\pm(r) \equiv -g|_{z=\pm\frac{h}{2}} - \mathcal{F}_z^\pm(\{\partial_z\phi|_{\partial\Omega}\}) = 0\end{aligned} \tag{5.17i, 5.17j}$$

$$\Delta_h\phi = g \tag{5.17k}$$

$$\begin{aligned}& \phi = \sigma_\phi(z) \qquad \text{at } r=1\\ & \Uparrow\\ & c_\phi(z) \equiv \left[\tfrac{1}{r}\partial_\theta\psi + \partial_{rz}\phi\right]\big|_{r=1} - \mathcal{F}_r(\{\partial_z\phi|_{\partial\Omega}\}) = 0\end{aligned} \tag{5.17l}$$

The major differences between the velocity and magnetic cases are the reduction from five to four in the number of elliptic problems, the time derivative in the magnetic compatibility equation, and the presence of the Dirichlet-to-Neumann mappings $\mathcal{F}_r$ and $\mathcal{F}_z^\pm$ which have replaced the normal derivatives of the exterior solution ϕ^{vac}. We recall the meaning of $\mathcal{F}_r(\{\partial_z\phi|_{\partial\Omega}\})$ and $\mathcal{F}_z^\pm(\{\partial_z\phi|_{\partial\Omega}\})$: the set $\{\partial_z\phi|_{\partial\Omega}\}$ provides Dirichlet boundary values for the exterior Laplace problem and $\mathcal{F}_r$ and $\mathcal{F}_z^\pm$ are the normal derivatives of the exterior solution at the boundaries.

The Dirichlet-to-Neumann mappings, as well as each solution and problem in (5.17), decouple according to azimuthal Fourier mode m and axial parity $p \in \{s,a\}$. As before, we construct the influence matrix by solving homogeneous versions of (5.17), with S_ψ and S_ϕ set to zero in (5.17a) and (5.17h) and a complete set of Dirichlet boundary values σ_f, σ_g, $\sigma_g^\pm$, σ_ϕ. Evaluating c_f, c_g, $c_g^\pm$, c_ϕ yields the influence matrix.

6. Conclusion

We have presented a poloidal–toroidal formulation for solving the time-dependent three-dimensional magnetohydrodynamic equations in a finite cylinder. While preserving the original mathematical formulation described in [1] and later tested on a linear stability Rayleigh–Bénard convection problem in [2], we incorporated the influence matrix technique [3] for decoupling the boundary and compatibility conditions emerging from the potential formulation. We have also described an extension of this algorithm to the induction equation governing the evolution of the magnetic field.

The most important advantage of using the toroidal–poloidal decomposition is that the divergence-free character of the velocity and magnetic fields is imposed exactly, by construction. For the induction equation, the potential formulation makes it possible to solve for the magnetic field without introducing an artificial numerical magnetic analogue of the hydrodynamic pressure. Although this quantity has no physical meaning, satisfactory results can nonetheless be obtained using such projection techniques [8–10]. Using scalar functions instead of components of vector fields simplifies and homogenizes the usage of differential operators. The influence matrix technique allows the poloidal–toroidal formulation to be sufficiently economical to be used for time-integration.

We have implemented and validated this method for the hydrodynamic von Kármán problem of flow in a cylinder driven by counter-rotating disks, using a spectral discretization which is regular on the cylindrical axis. These results are presented in a companion article [26]. In extending this algorithm to the full magnetohydrodynamic problem, no difficulty is posed by the induction equation, whose structure is simpler than that of the Navier–Stokes equation. Instead, the main difficulty is that the magnetic field is not specified at the domain boundary but must instead satisfy matching conditions between the interior domain (here a finite cylinder) and the exterior domain (here an infinite vacuum). We have developed a formalism involving the Dirichlet-to-Neumann mapping for eliminating the exterior magnetic field, which has been implemented and validated for a two-dimensional test problem [32]. Future research will focus on implementing the poloidal–toroidal formulation for the full magnetohydrodynamic problem.

Acknowledgments

The simulations reported in this work were performed on the IBM Power 4 of the Institut de Développement et des Ressources en Informatique Scientifique (IDRIS) of the Centre National de la Recherche Scientifique (CNRS) as part of project 1119. P.B. was supported by a doctoral and post-doctoral grant from the Ecole Doctorale of the Ecole Polytechnique and the Ministère de l'Education Nationale, de la Recherche et de la Technologie (MENRT).

Appendix A. Regularizing the influence matrix

In Section 4.3, we have assumed that the influence matrices $\mathcal{C}^{pm}$ are invertible, which is actually not the case. The influence matrices are non-invertible for several reasons. The first issue is geometric. The finite cylinder has corners at which conditions at $z = \pm\frac{h}{2}$ and $r = 1$ must both be satisfied. When formulated in spectral rather than physical space, the redundant conditions correspond to a linear combination of rows and cannot be easily identified. A second factor is the discretization of the Poisson and Helmholtz solvers, in particular the replacement of the highest-wavenumber equations by the boundary conditions mandated by the τ method. A third cause is the decrease in polynomial order due to differentiation by boundary operators. For numerical reasons, the eigenvalues corresponding to these directions may be nearly zero, rather than exactly so.

One remedy [3,6] consists of thresholding: diagonalizing $\mathcal{C}^{pm}$ and replacing the eigenvalues whose absolute values are below a certain experimentally determined threshold ϵ_μ by an arbitrary value, say 1, leading to an invertible matrix. The justification of this manipulation of the spectrum is that the eigenvectors corresponding to the zero eigenvalues play no role in satisfaction of the boundary conditions. This is true if the linear system of equations defined by the influence matrix and the right-hand-side is underdetermined, i.e. if the right-hand-side belongs to the image space of the influence matrix. Because the particular solutions are determined using the same nested solver used for constructing the homogeneous solutions, this is in fact the case.

However, a major problem remains. Even after eigenvalues are eliminated which would be exactly zero if infinite precision were used, the resulting matrices still have very small eigenvalues, i.e. they are still poorly conditioned. There are various causes for this. Some boundary value distributions are almost linearly dependent. More importantly, because some boundary conditions are of higher differential order then others, the magnitudes of different portions of the influence matrices are very different. We shall call these eigenvalues *small*, in contrast to those which would be zero in infinite precision, which we shall call simply zero eigenvalues. The small eigenvalues depend on the spatial resolution and on the product $Re/\delta t$, a parameter which appears in the Helmholtz problem. As the resolution or $Re/\delta t$ are increased, an increasing number of small eigenvalues appear, whereas the number of zero eigenvalues depends only on the geometry and on the kind of boundary conditions.

The condition number, approximately the ratio between the largest and smallest eigenvalues values of a matrix, is an upper bound on the number of lost meaningful digits in the numerical solution to a linear equation involving this matrix. If the threshold ϵ_μ is chosen such as to lower the condition number to an acceptable value ($O(10^8) - O(10^{10})$), then small eigenvalues are eliminated, in addition to zero eigenvalues, leading to errors in satisfaction of the boundary conditions that are much higher than machine precision. The challenge is, first, to distinguish between the zero and small eigenvalues so as to eliminate only the zero eigenvalues and, second, to improve the condition number of the adjusted matrix in some way other than by eliminating the small eigenvalues.

We first modified the thresholding procedure by using the singular value decomposition (SVD) rather than diagonalization. The advantages of the SVD is, first, that it always exists and, second, that the matrix of singular vectors is better conditioned than the eigenvector matrix, because the left and right singular vectors are orthogonal, in contrast to eigenvectors, which may be close to linearly dependent. As an example, we consider the influence matrix for spatial resolution $(N = 96) \times (K = 192)$, Reynolds number $Re = 10^4$ and time step $\delta t = 10^{-2}$. The magnitudes of the singular values γ_i of the influence matrix block $\mathcal{C}^{1,s}$ with azimuthal Fourier wavenumber $m = 1$ and axial parity $p = s$ are presented on Fig. 3a. $\mathcal{C}^{1,s}$ has one zero singular value (i.e. a singular value which would be exactly zero in infinite precision). Fig. 3(left) shows that this value is numerically 10^{-21}, separated from the next smallest singular value. In contrast, the zero eigenvalue and smallest remaining eigenvalue are of the same size and hence cannot be distinguished. However, thresholding, whether by replacing this singular value or the corresponding eigenvalue, still leaves the condition number unacceptably high, on the order of $10^6/10^{-15} = 10^{20}$ for this example.

The matrix condition number can be decreased more effectively by scaling prior to thresholding. If each row is divided by its norm, the condition number of the matrix is significantly reduced, down to 10^{11} for $m > 0$ and below 10^8 for $m = 0$. Additional scaling of columns does not significantly change the condition number. The

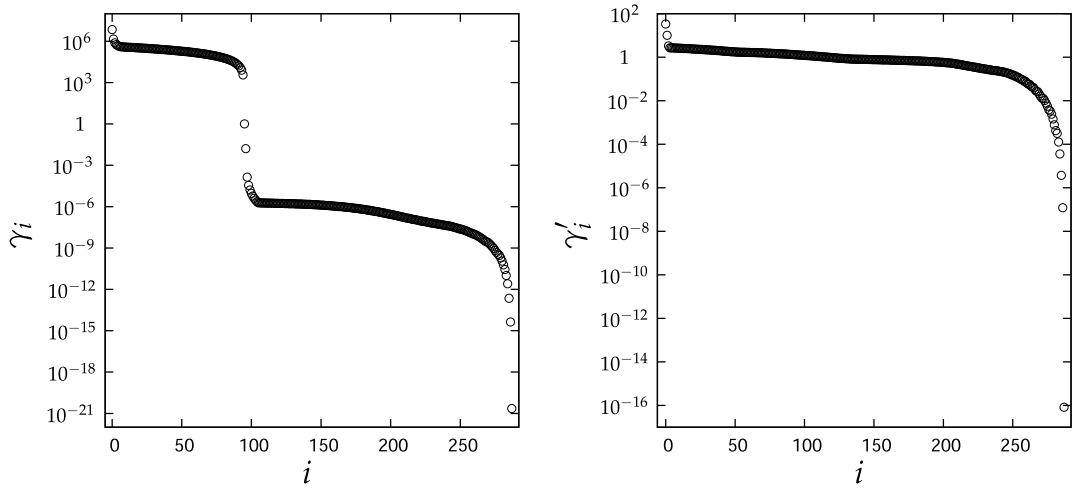

Fig. 3. Singular values $\{\gamma_i\}$ for case with $(N = 96) \times (K = 192)$, $Re/\delta t = 10^6$, $m = 1$, $p = s$. Left: original influence matrix $\mathcal{C}^{1,s}$. Right: scaled influence matrix $(\mathcal{C}^{1,s})' \equiv [\boldsymbol{\alpha}]\mathcal{C}^{1,s}[\boldsymbol{\beta}]$.

condition number of the $m = 0$ matrices are sufficiently decreased by scaling only their rows, because their poloidal and toroidal potentials are not coupled. For $m > 0$, the influence matrices can be further improved by scaling blocks corresponding to different combinations of types of test functions and boundary conditions. The influence matrices $\mathcal{C}^{pm}$ for $m > 0$ are composed of nine submatrices: the three columns correspond to the three types of imposed simplified Dirichlet boundary conditions $\{\sigma_g(z), \sigma_f(z), \sigma_g^{\pm}(r)\}$ while the three rows correspond to the three quantities $\{c_g(z), c_f(z), c_g^{\pm}(r)\}$ reflecting the actual boundary conditions. We represent the $|\cdot|_\infty$ norm of the corresponding submatrix of $\mathcal{C}^{pm}$ by c_{ij}, where, for example, c_{12} designates the norm of the (c_g,σ_f) submatrix.

For the resolution $(N = 96) \times (K = 192)$, the matrix norms c_{ij} of each of the blocks are:

$$\mathcal{C}^{1,s} = \left[\begin{array}{c|c|c} c_{11} & c_{12} & c_{13} \\ \hline c_{21} & c_{22} & c_{23} \\ \hline c_{31} & c_{32} & c_{33} \end{array}\right] = \left[\begin{array}{c|c|c} 10^{7} & 1 & 1 \\ \hline 10^{-2} & 10^{-5} & 10^{-5} \\ \hline 0 & 10^{-5} & 10^{-4} \end{array}\right] \tag{A.1}$$

We now wish to scale the block-rows and block-columns in such a way as to make the norms c'_{ji} of the resulting scaled blocks equal to one another.

$$[\boldsymbol{\alpha}]\,\mathcal{C}^{1,s}\,[\boldsymbol{\beta}] = \left[\begin{array}{c|c|c} \alpha_1 & 0 & 0 \\ \hline 0 & \alpha_2 & 0 \\ \hline 0 & 0 & \alpha_3 \end{array}\right] \left[\begin{array}{c|c|c} c_{11} & c_{12} & c_{13} \\ \hline c_{21} & c_{22} & c_{23} \\ \hline 0 & c_{32} & c_{33} \end{array}\right] \left[\begin{array}{c|c|c} \beta_1 & 0 & 0 \\ \hline 0 & \beta_2 & 0 \\ \hline 0 & 0 & \beta_3 \end{array}\right] = \left[\begin{array}{c|c|c} c'_{11} & c'_{12} & c'_{13} \\ \hline c'_{21} & c'_{22} & c'_{23} \\ \hline 0 & c'_{32} & c'_{33} \end{array}\right] \tag{A.2}$$

In general there exist no $\{\alpha_i\}$ and $\{\beta_i\}$ satisfying $c'_{11} = c'_{12} = c'_{13} = c'_{21} = c'_{22} = c'_{23} = c'_{32} = c'_{33} = 1$. We can instead require

$$\begin{aligned} &\alpha_1\beta_1 c_{11} = \alpha_2\beta_2 c_{22} = \alpha_3\beta_3 c_{33} = 1 \\ &\alpha_2\beta_1 c_{21} = \alpha_1\beta_2 c_{12} \\ &\alpha_3\beta_1 c_{31} = \alpha_1\beta_3 c_{13} \end{aligned} \tag{A.3}$$

The system (A.3) has an infinite number of possible solutions, from which we can select the following:

$$\begin{aligned} &\alpha_1 = \sqrt{\tfrac{c_{21}c_{32}c_{33}}{c_{11}c_{12}c_{23}}} \quad \alpha_2 = \sqrt{\tfrac{c_{32}c_{33}}{c_{22}c_{23}}} \quad \alpha_3 = 1 \\ &\beta_1 = \sqrt{\tfrac{c_{11}c_{23}}{c_{11}c_{21}c_{32}c_{33}}} \quad \beta_2 = \sqrt{\tfrac{c_{23}}{c_{22}c_{32}c_{33}}} \quad \beta_3 = \tfrac{1}{c_{33}} \end{aligned} \tag{A.4}$$

After scaling using (A.2)–(A.4), the influence matrix $\mathcal{C}^{1,s}$ has the following structure:

$$\mathcal{C}^{1,s'} = \left[\begin{array}{c|c|c} c'_{11} & c'_{12} & c'_{13} \\ \hline c'_{21} & c'_{22} & c'_{23} \\ \hline c'_{31} & c'_{32} & c'_{33} \end{array}\right] = \left[\begin{array}{c|c|c} 1 & 10^{-2} & 10^{-2} \\ \hline 10^{-2} & 1 & 1 \\ \hline 0 & 1 & 1 \end{array}\right] \tag{A.5}$$

The zero singular value is then easily identified and replaced by 1, leading to a condition number of 10^{11}, like that for simple row or column scaling. But if the block scaling is followed by row scaling and then replacement of the zero singular value, then the condition number is further reduced to the acceptable value of 10^8. The singular values of the matrix after block and row scaling are presented on Fig. 3(right).

We note that operators with high condition numbers are inherent in the numerical discretization of partial differential equations; for example, the 1D second derivative operator with homogeneous boundary conditions using a basis of K Chebyshev polynomials and corresponding grid has condition number $O(K^4)$. The requirements for the solution of the linear systems that occur in this context are not those of numerical linear algebra:

the right-hand-side is not arbitrary, but results from time-integration, and not all components are of equal weight. In our case, we find that after an initial small integration time of $T = 100\ \delta t$, the right-hand-side is always such that the influence matrix, scaled and regularized to reduce its condition number to $O(10^8)$, can be inverted to satisfy the constraints in system (4.3) to machine accuracy [26].

One welcome consequence of scaling is that it separates the zero singular values which result from non-invertibility of the matrix from the small singular values which result from poor conditioning of the various components of the influence matrix. Without scaling, the number of singular values below a fixed threshold depends on the spatial resolution and so the zero eigenvalues cannot be reliably identified and removed. More importantly, scaling vastly improves the condition number of the influence matrix, insuring satisfaction of the constraints to machine accuracy.

References

[1] F. Marques, On boundary conditions for velocity potentials in confined flows: application to Couette flow, Phys. Fluids A 2 (1990) 729.
[2] F. Marques, M. Net, J.M. Massaguer, I. Mercader, Thermal convection in vertical cylinders. A method based on potentials, Comput. Methods Appl. Mech. Eng. 110 (1993) 157–169.
[3] L.S. Tuckerman, Divergence-free velocity fields in nonperiodic geometries, J. Comput. Phys. 80 (1989) 403–441.
[4] D. Rempfer, On boundary conditions for incompressible Navier–Stokes problems, Appl. Mech. Rev. 59 (2006) 107–125.
[5] P.S. Marcus, Simulation of Taylor–Couette flow. I. Numerical methods and comparison with experiment, J. Fluid Mech. 146 (1984) 65–113.
[6] M.F.M. Speetjens, H.J.H. Clercx, A spectral solver for the Navier–Stokes equations in the velocity–vorticity formulation, Int. J. Comput. Fluid Dyn. 19 (2005) 191–209.
[7] J.M. Lopez, F. Marques, J. Shen, An efficient spectral-projection method for the Navier–Stokes equations in cylindrical geometries – three-dimensional cases, J. Comput. Phys. 176 (2002) 384–401.
[8] J.U. Brackbill, D.C. Barnes, The effect of nonzero $\nabla \cdot B$ on the numerical solution of the magnetohydrodynamic equations, J. Comput. Phys. 35 (1980) 426.
[9] K. Chan, K. Zhang, J. Zou, G. Schubert, A non-linear 3D spherical α^2 dynamo using a finite element method, Phys. Earth Planet. Int. 128 (2001) 35–50.
[10] G. Tóth, The $\nabla \cdot B = 0$ constraint in shock-capturing magnetohydrodynamics codes, J. Comput. Phys. 161 (2000) 605–652.
[11] P.S. Marcus, Effects of truncation in modal representations of thermal convection, J. Fluid Mech. 103 (1981) 241–255.
[12] G.A. Glatzmaier, Numerical simulation of stellar convective dynamos. 1. The model and method, J. Comput. Phys. 55 (1984) 461–484.
[13] M. Dudley, R. James, Time-dependent kinematic dynamos with stationary flows, Proc. Roy. Soc. London A 425 (1989) 407–429.
[14] G.A. Glatzmaier, P.H. Roberts, A three-dimensional self-consistent computer simulation of a geomagnetic field reversal, Nature 337 (1995) 203.
[15] A. Tilgner, A kinematic dynamo with a small scale velocity field, Phys. Rev. A 226 (1997) 75–79.
[16] R. Hollerbach, A spectral solution of the magneto-convection equations in spherical geometry, Int. J. Num. Methods Fluids 32 (2000) 773.
[17] H.B. Squire, On the stability for three-dimensional disturbances of viscous flow between parallel walls, Proc. Roy. Soc. Lond. A 142 (1933) 621.
[18] P.J. Schmid, D.S. Henningson, Stability and Transition in Shear Flows, Springer, 2001.
[19] J. Antonijoan, F. Marques, J. Sanchez, Non-linear spirals in the Taylor–Couette problem, Phys. Fluids 10 (1998) 829.
[20] A.P. Willis, C.F. Barenghi, Hydromagnetic Taylor–Couette flow: numerical formulation and comparison with experiment, J. Fluid Mech. 463 (2002) 361–475.
[21] T. von Kármán, Uber laminäre und turbulente Reibung, Z. Angew. Math. Mech. 1 (1921) 233–252.
[22] M. Bourgoin, L. Marié, F. Petrelis, C. Gasquet, A. Guigon, J.B. Luciani, M. Mulin, F. Namer, J. Burgete, A. Chiffaudel, F. Daviaud, S. Fauve, P. Odier, J.F. Pinton, Magnetohydrodynamics measurements in the von Kármán sodium experiment, Phys. Fluids 14 (2002) 3046.
[23] C. Nore, L.S. Tuckerman, O. Daube, S. Xin, The 1:2 mode interaction in exactly counter-rotating von Kármán swirling flow, J. Fluid Mech. 477 (2003) 51–88.
[24] P. Boronski, A method based on poloidal–toroidal potentials applied to the von Kármán Flow in a finite cylinder geometry, Ph.D. Thesis, Ecole Polytechnique, 2005.
[25] T. Matsushima, P.S. Marcus, A spectral method for polar coordinates, J. Comput. Phys. 120 (1995) 365.
[26] P. Boronski, L.S. Tuckerman, Poloidal–toroidal decomposition in a finite cylinder: II. Discretization, regularization and validation, J. Comput. Phys, this issue, doi:10.1016/j.jcp.2007.08.035.
[27] W. Dobler, K.H. Rädler, An integral equation approach to kinematic dynamo models, Geophys. Astrophys. Fluid Dyn. 89 (1998) 45–47.
[28] A.B. Iskakov, S. Descombes, E. Dormy, An integro-differential formulation for magnetic induction in bounded domains: boundary element-finite volume method, J. Comput. Phys. 7 (2004) 540–554.

[29] A.B. Iskakov, E. Dormy, On magnetic boundary conditions for non-spectral dynamo simulations, Geophys. Astrophys. Fluid Dyn. 99 (2005) 481–492.
[30] M. Xu, F. Stefani, G. Gerbeth, The integral equation method for a steady kinematic dynamo problem, J. Comput. Phys. 196 (2004) 102–125.
[31] J.L. Guermond, R. Laguerre, J. Léorat, C. Nore, An interior penalty Galerkin method for the MHD equations in heterogeneous domains, J. Comput. Phys. 221 (2007) 349–369.
[32] P. Boronski, Spectral method for matching exterior and interior elliptic problems, J. Comput. Phys. 225 (2007) 449–463.